# CFD SIMULATION OF A CO-ROTATING TWIN-SCREW EXTRUDER: VALIDATION OF A RHEOLOGICAL MODEL FOR A STARCH-BASED DOUGH FOR SNACK FOOD

**Giorgia Tagliavini[(a)], Federico Solari[(b)], Roberto Montanari[(c)]**

[(a)] CIPACK Interdepartmental Center, University of Parma – Parco Area delle Scienze, 43124 Parma (Italy)
[(b), (c)] Department of Industrial Engineering, University of Parma – Parco Area delle Scienze, 43124 Parma (Italy)

[(a)]giorgia.tagliavini@unipr.it, [(b)]federico.solari@unipr.it, [(c)]roberto.montanari@unipr.it

**ABSTRACT**
The extrusion of starch-based products has been a matter of interest, especially for the pasta and snack food production. In recent years, twin-screw extruders for snack food were studied from both structural and fluid dynamics viewpoints.
This project started from the rheological characterization of a starch-based dough (corn 34wt%, tapioca 32wt%), comparing viscosity values acquired in laboratory with different theoretical models found in literature.
A CFD simulation recreating the simple case of a fluid flow between two parallel plates was carried out in order to validate the former comparison. After the rheological characterization was completed, the second phase of this work covered a 3D CFD simulation of the first part of the twin-screw extruder (feeding zone).
The objective was to find a suitable model for describing the dough rheological behavior and the operating conditions of a co-rotating intermeshing twin-screw extruder.
Once the model would be design, it would allow to investigate several working conditions and different screws geometries of the machine, predicting the evolution of the product rheological properties.

Keywords: twin-screw extruders, starch-based dough, computational fluid-dynamics, rheological model

## 1. INTRODUCTION

In the food industry, the extrusion of starch-based doughs has been widely studied.
One of these doughs main features is the non-Newtonian behavior, which is characterized by changes in the rheological properties depending on the undergoing process (Pessini, 2001). These rheological changes are affected by temperature, shear stress and shear rate (Lagarrigue & Alvarez, 2001), moisture content (Rao et al., 1997) and other occurring substances inside the dough (Xei et al., 2009; Jamilah et al., 2009).
All these factors are thus crucial in terms of obtaining the desired product.

Extrusion is a technique employed for quite some time especially in the food industry. It consists in the conveying of high viscosity fluids by increasing the pressure from the hopper towards the extruder die. Extruders can be divided in three key zones: a feeding zone, a plasticization zone and a metering zone (as shown in Figure 1).

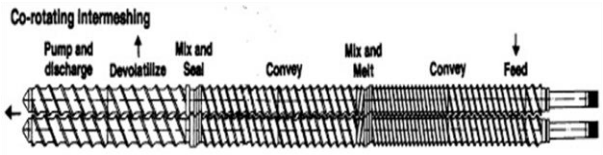


Figure 1: Simplified scheme of a co-rotating intermeshing twin-screw extruder (modified from: http://plastictechnologies.blogspot.de).

The extruder may also be a single- or twin-screw: in the latter, the two parallel screws can co-rotate or counter-rotate, according to the pressure needed (Messori 2005).
A co-rotating twin-screw extruder provides a more accurate regulation on the process and a higher range of shear stresses (and of shear rate as a result).
In the food industry the main goal is to achieve smooth and homogeneous products, reason why twin-screw extruders are preferred over single-screw ones.
Nevertheless, inside twin-screw extruders, it is more complicated to evaluate the fluid dynamics behavior and the share rate distribution. For this reason, fluid dynamics simulations are essential especially in the design phase.
In the last decade, twin-screw extruders for snack food were studied from both structural (with finite element method) and fluid-dynamics (with CFD simulations) perspectives (Yamsaengsung et al., 2010; Fabbri et al., 2012; Cubeddu et al., 2014; Bertrand et al., 2003).
In recent years, computational fluid dynamics (CFD) has been gaining highlights for predicting fluid dynamic behavior for a wide range of industrial processes.
The objective of this work is the rheological characterization of a starch dough for snack food and the design of a CFD model with ANSYS FLUENT 17.0 of a twin-screw extruder first section (feeding zone).

## 2. MATERIALS AND METHODS

### 2.1. Data collection

The first step of this work started with laboratory measurements, collecting the viscosity data of the product at known shear rates.

The instrumentation used for the data collection consisted in a Brookfield Engineering RST Controlled Stress Rheometer (RST-CC Coaxial Cylinder model). The rheometer and the spindle technical specifications are listed in Table 1 and Table 2.

Table 1: RST-CC rheometer technical specifications.

| | |
|---|---|
| Viscosity Range [Pa·s] | 0.00005 – 5.41M |
| Speed [rpm] | 0.01 – 1.3K |
| Max. Torque [mNm] | 100 |
| Torque Res. [µNm] | 0.15 |

Table 2: CCT-25 spindle technical specifications.

| | |
|---|---|
| Viscosity Range [Pa·s] | 0.002 – 177K |
| Shear Rate [$s^{-1}$] | 0.013 – 1.67K |
| Max. Shear Stress [Pa] | 2.28K |
| Sample Volume [mL] | 16.8 |

The viscosity values and the associated shear rates collected during the laboratory campaign are shown in Table 3.

Table 3: Collected data from laboratory tests.

| Shear Rate [$s^{-1}$] | Viscosity [Pa·s] |
|---|---|
| 4.5 | 0.171 |
| 7.47 | 0.167 |
| 12.51 | 0.158 |
| 20.88 | 0.137 |
| 40.77 | 0.115 |
| 58.05 | 0.104 |

### 2.2. Rheological models

The next step was the rheological characterization of the starch dough (corn 34wt%, tapioca 32wt%).

As mentioned before, one of these doughs main features is the non-Newtonian behavior, which implies changes in the rheological properties, depending on the extrusion conditions.

For Newtonian fluids, the shear stress is described by Equation 1, as a function of the rate-of-deformation tensor $\overline{\overline{D}}$:

$$\overline{\overline{\tau}} = \mu \overline{\overline{D}} \tag{1}$$

where $\mu$ is the viscosity, which is independent of $\overline{\overline{D}}$. $\overline{\overline{D}}$ is defined by Equation 2 as:

$$\overline{\overline{D}} = \left( \frac{\partial u_j}{\partial x_i} + \frac{\partial u_i}{\partial x_j} \right) \tag{2}$$

where $u$ and $x$ are the velocity and the coordinate respectively.

The situation is different when it comes to non-Newtonian fluids. In this case, there is a dependence between the viscosity $\eta$ (non-Newtonian viscosity) and the rate-of-deformation tensor $\overline{\overline{D}}$ (Equation 3):

$$\overline{\overline{\tau}} = \eta(\overline{\overline{D}})\overline{\overline{D}} \tag{3}.$$

In relation to this study case, the viscosity $\eta$ depends only on the shear rate $\dot{\gamma}$, which is related to the tensor $\overline{\overline{D}}$ according to the following equation:

$$\dot{\gamma} = \sqrt{\frac{1}{2}\overline{\overline{D}} : \overline{\overline{D}}} \tag{4}.$$

For simplification purposes, the temperature effects on viscosity were omitted at this first stages.

The related terms will, therefore, not be shown in the following equations.

An extensive bibliographic research revealed that the most commonly used models for describing starch-based fluids are the non-Newtonian Power Law, the Carreau and the Cross model (Emin & Schuchmann, 2012).

The governing equations of the models mentioned above are described below, in accordance with the formulation presented in the ANSYS FLUENT *Theory Guide* (Ansys, Inc., 2009).

#### 2.2.1. Power Law for non-Newtonian Viscosity

A non-Newtonian flow is modeled with Equation 5, according to the power law for the non-Newtonian viscosity:

$$\eta = K\dot{\gamma}^{n-1} \tag{5}$$

where $K$ is the consistency index, $n$ is the power law index, a measure of the average viscosity of the fluid and a measure of the fluid deviation from Newtonian behavior respectively, which define the fluid classes:

- $n = 1 \rightarrow$ Newtonian fluid;
- $n > 1 \rightarrow$ shear-thickening (dilatant fluid);
- $n < 1 \rightarrow$ shear-thinning (pseudo-plastic).

#### 2.2.2. The Carreau Model for pseudo-plastics

The power law model described in Equation 5 results in a fluid viscosity that varies with shear rate.

The Carreau model attempts to describe a wide range of fluids thanks to a curve-fit, which synthetizes functions for both Newtonian and shear-thinning non-Newtonian laws. In the Carreau model, the viscosity is:

$$\eta = \eta_\infty + (\eta_0 - \eta_\infty)[1 + \dot{\gamma}^2\lambda^2]^{(n-1)/2} \quad (6)$$

where the parameters $n$, $\lambda$, $\eta_0$ and $\eta_\infty$ depend upon the fluid. $\lambda$ is the time constant, $n$ is the power law index, $\eta_0$ and $\eta_\infty$ are respectively the zero- and the infinite-shear viscosities. The viscosity is limited by $\eta_0$ for $\dot{\gamma} \to 0$ and by $\eta_\infty$ for $\dot{\gamma} \to \infty$.

### 2.2.3. The Cross Model

The Cross model for viscosity is:

$$\eta = \frac{\eta_0}{1 + (\lambda\dot{\gamma})^{1-n}} \quad (7).$$

$\eta_0$ is the zero-shear viscosity, $\lambda$ is the natural time (i.e., inverse of the shear rate at which the fluid changes from Newtonian to power-law behavior) and $n$ is the power law index.

### 2.3. Data processing and analysis

The data were processed with Microsoft Office Excel 2013.
The experimental viscosities were used to derive the coefficients of the rheological models by minimizing the mean squared error between the experimental results and those obtained using Equations 5, 6 and 7.
Then the coefficient of determination $R^2$ was estimated.
This was a fundamental step for the continuation of the study, since the coefficients values are required by the CFD simulation software for the fluid characterization.
The results are shown in Tables 4 and 5 and Figure 3.

Table 4: Viscosity values.

| Viscosity [Pa·s] | | | |
|---|---|---|---|
| Lab tests | Power Law | Carreau | Cross |
| 0.171 | 0.179 | 0.172 | 0.173 |
| 0.167 | 0.163 | 0.166 | 0.165 |
| 0.158 | 0.148 | 0.155 | 0.154 |
| 0.137 | 0.134 | 0.139 | 0.140 |
| 0.115 | 0.118 | 0.115 | 0.116 |
| 0.104 | 0.110 | 0.103 | 0.102 |

Table 5: Coefficients and $R^2$ values.

| | Power Law | Carreau | Cross |
|---|---|---|---|
| $K$ | 0.239 | | |
| $n$ | 0.809 | 0.635 | 0.129 |
| $\lambda$ | | 0.083 | 0.014 |
| $\eta_0$ | | 0.176 | 0.189 |
| $\eta_\infty$ | | 0.011 | |
| $R^2$ | 0.936 | 0.997 | 0.991 |

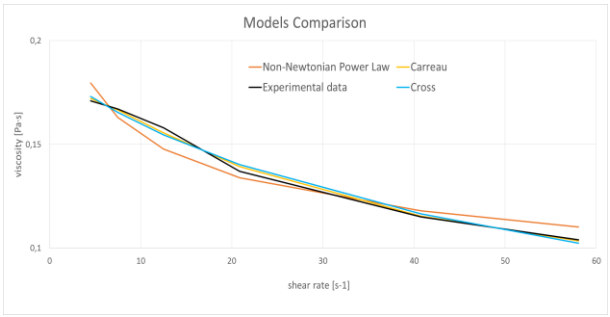


Figure 2: Models comparison from the Microsoft Office Excel elaboration.

## 3. CFD SIMULATION FOR RHEOLOGICAL MODELS VALIDATION

A CFD simulation was helpful to identify the most suitable rheological model among the ones mentioned previously. A 2D geometry was implemented in ANSYS FLUENT, recreating the simple case of a fluid flow between two fixed, parallel plates.
Figure 3 shows a detail of the 2D fluid domain used in the simulation.


Figure 3: 2D computational domain with inlet velocity.

The length, in particular, was extended at 5 m to get a fully-developed flow inside the duct.
The domain sizes are presented in Table 6, while Table 7 lists the mesh specification.

Table 6: Domain sizes.

| | Size [m] |
|---|---|
| Height (D) | 0.1 |
| Length (L) | 5 |

The domain was decomposed with ANSYS MESHING, according to the Finite Element Method.
Table 7 lists the mesh specifications.

Table 7: Mesh specifications.

| Element Type | Quadrilaterals |
|---|---|
| Num. Elements | 5240 |
| Num. Nodes | 5523 |
| Min. Size | 0.0025 m |
| Max. Size | 0.498 m |
| Max. Face Size | 0.249 m |
| Wall Edge Sizing | Num. of division: 250 |
| Inlet/Outlet Edge Sizing | Num. of division: 20 |

Three different simulations (one for each rheological model) were carried out in ANSYS FLUENT 17.0 with stationary operating conditions.
The inlet velocity was fixed at 2.5 m/s and the atmospheric pressure was set at the outlet.

For the fluid characterization, the software requires the coefficients of the chosen model and the density. The models' coefficients and a density of 588.94 kg/m$^3$ were implemented in the simulator.
The fluid flow was set as laminar, due to the high viscosity of the product.

### 3.1. Results

The aim of this phase was finding the model that best fits the experimental data.
First, the viscosity values were observed with the contour using CFD-Post software.
The results are shown in Figures 4 and 5.

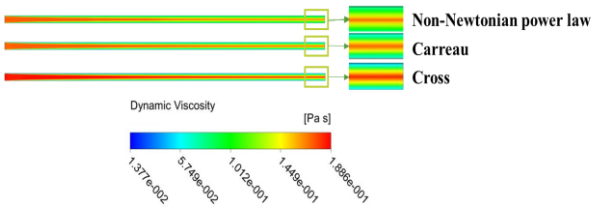


Figure 4: Dynamic viscosity contour comparison between rheological models.

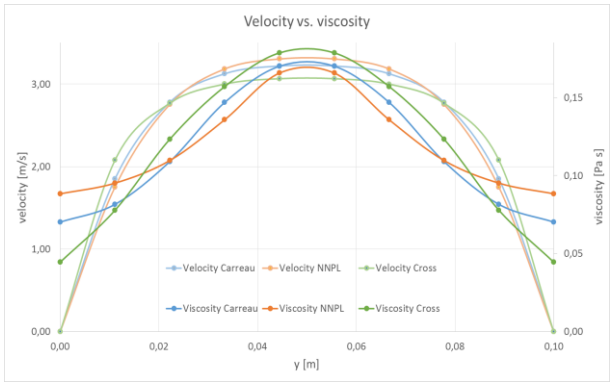


Figure 5: Comparative graph with velocity and viscosity values for different rheological model, depending upon duct height.

The profiles shown in Figure 5 are dependent upon the domain height and reveal how well each model reproduce the fluid behavior in terms of velocity and viscosity.
Afterwards, the viscosity values were plotted as a function of the shear rate together with the experimental data. The shear rate was solved taking the derivative of the velocity in $\partial y$.
This approach allows to see which model implemented in the software would be more accurate.
Finally, the viscosities were put together in the same graph as a function of $\partial v/\partial y$ [s$^{-1}$].
Figure 6 illustrates the results.

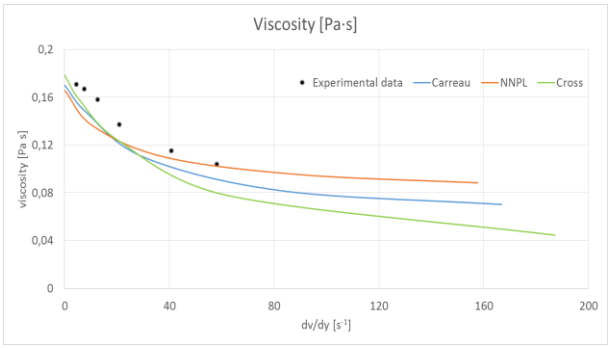


Figure 6: Comparison between the viscosity simulation and experimental data as a function of shear rate.

The values reveal that the most suitable model was the Carreau one.
The non-Newtonian Power Law marks the experimental data quite well, while the Cross model was the less appropriate.

## 4. CFD SIMULATION OF THE TWIN-SCREW EXTRUDER

The second phase of the study began with 3D modeling of the twin-screw extruder (feeding zone section).
The geometry reproduced the layout of the extruder's first section of the pilot plant, on which the experimental tests will be carried out to collect a further amount of data for future validation.
Figure 7 shows the size of the model and Figure 8 depicts the 3D geometry.

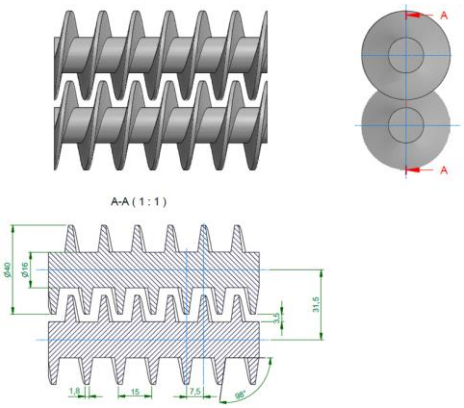


Figure 7: Extruder sizes in (m).

Figure 8: 3D geometry of the twin-screw extruder implemented in ANSYS FLUENT 17.0.

The designed geometry defining the computational fluid volume was decomposed with ANSYS MESHING, according to the Finite Element Method.
Special attention was paid to the creation of the mesh, in order to have accurate information about fluid dynamic behavior in near-wall regions and in leakage areas. Actually, there are narrow gaps between the screws and between the screw threads and the barrel. Hence, an inflated mesh is required in those areas to prevent the lack of details during the calculation.
Furthermore, a dedicated mesh was generated for the boundary layer in connection with the solid parts (barrel and screws walls).
Table 8 and Figure 9 show the mesh structure and specifications.

Table 8: Extruder mesh specifications.

| Element type | Volume: tetrahedrons |
|---|---|
| | Boundary: quadrilaterals |
| Num. Elements | 2721599 |
| Num. Nodes | 9259878 |
| Min. Size | $8 \cdot 10^{-5}$ m |
| Max. Size | $1 \cdot 10^{-3}$ m |
| Max. Face Size | $1 \cdot 10^{-3}$ m |
| Inflation (boundary layer) | Total thickness |
| | Num. of layers: 4 |
| | Max thickness: $1 \cdot 10^{-4}$ m |
| Threads sizing | $2 \cdot 10^{-4}$ m |
| Screw sizing | $6 \cdot 10^{-4}$ m |
| Barrel sizing | $8 \cdot 10^{-4}$ m |
| Edge sizing | $4 \cdot 10^{-4}$ m |

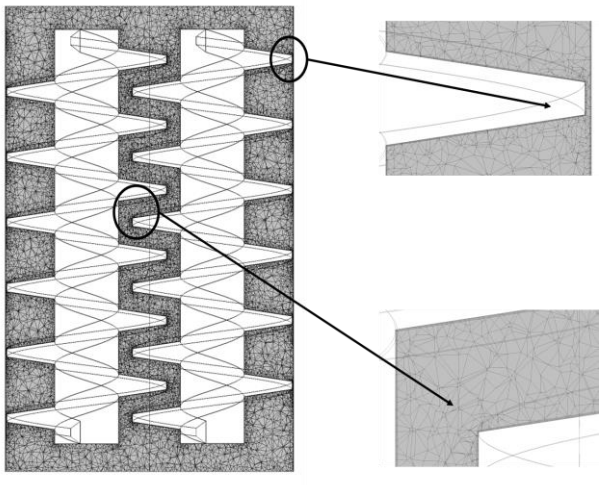

Figure 9: Mesh structure with details of near-wall region and leakage areas.

The simulation was carried out in a transient state to stress the influence of the screw rotation on the flow behavior. The fluid parameters are those used in the 2D simulation, i.e. the Carreau model and the laminar flow regime.

The atmospheric pressure was set at the inlet, so that the fluid flow would be influence solely by the screw rotation. A sharp restriction at the outlet cross-section (not shown in Figure 8) was imposed to reproduce the pressure drop caused by the machine consecutive zones.
To impose the angular velocity of 370 rpm a UDF in C language was created and compiled inside ANSYS FLUENT.
To recreate the screws rotation the dynamic mesh option was chosen. This method allows a partition of the mesh in motion zones, remeshing zones and static zones.
The remeshing zone are the areas where the mesh is rebuilt following the solid parts rotation step by step during the calculation.
In the present case, before starting to create the dynamic mesh zones, the fluid domain was split into several parts. Specifically, the boundary layer related to the screws and the barrel walls was separated from the rest of the fluid domain.
In this way the fluid volume was divided into 4 regions. The areas created by the dynamic mesh are illustrated in Table 9.
The term "*rigid body*" specifies the moving zones, "*deforming*" the zones affected by the remeshing process and "*stationary*" the fixed zones, not subjected to remeshing.

Table 9: Dynamic mesh zones.

| Screws | Rigid body |
|---|---|
| Screws boundary layer | Rigid body |
| Barrel wall | Stationary |
| Barrel wall boundary layer | Stationary |
| Inlet | Stationary |
| Inlet boundary layer | Stationary |
| Outlet | Stationary |
| Outlet boundary layer | Stationary |
| Extruder interior | Deforming |

Therefore, the dynamic mesh allows the various boundary layers to move together with its corresponding wall, so as to facilitate the remeshing operation confining it to tetrahedral elements, which are easier to manage.
The simulation time was chosen in accordance with the real dough's residence time inside the machine.

### 4.1. Results

Once the simulations ended, velocity and viscosity values were observed.
The velocity vectors (Figure 10) show how the product is conveyed only by the screws' rotation. This agrees with the real case and with the boundary conditions entered in the software.

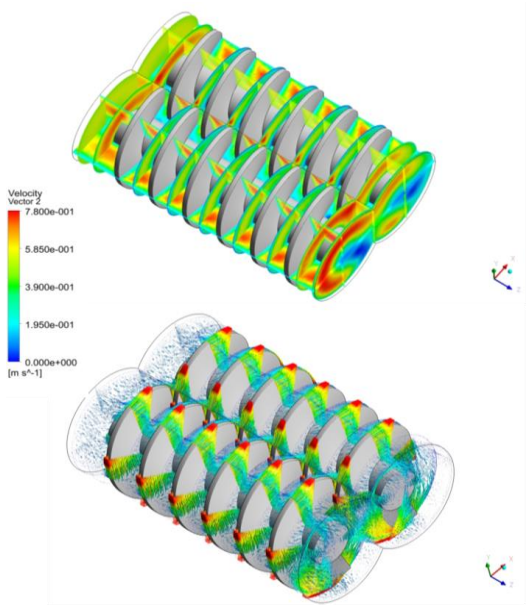


Figure 10: Velocity module and vectors. The fluid flows along the z-positive direction.

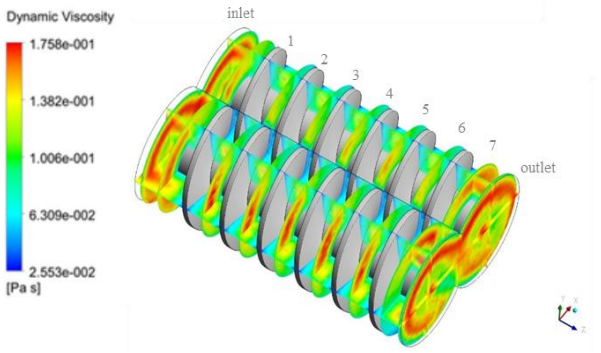


Figure 11: Viscosity contour.

Observing values of the dynamic viscosity in Figure 11, it is evident how they agree with the ones found in Table 4, for the laboratory results.

In Figure 11 the sampling sections are shown, from which the viscosity values were calculated as reported in the graph in Figure 12.

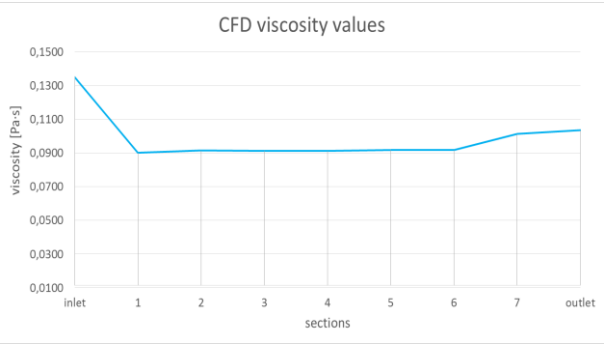


Figure 12: Viscosity values as function of the sampling sections.

## 5. CONCLUSIONS

This work has both the objective to find a rheological model for a corn and tapioca dough used for snack food and to design a 3D computational model, which could recreate the operating conditions of a co-rotating twin-screw extruder.

A set of viscosity values was obtained experimentally at specific shear rates.

The experimental data were then compared with the theoretical viscosity from non-Newtonian Power Law, Carreau and Cross models, which equations are often used for describing non-Newtonian fluid behavior.

To find which model was the most suitable, a simple 2D geometry of two parallel flat planes was created. Three simulations were carried out with this geometry and it turned out that the Carreau model was the one that best reproduced the trend of the experimental values.

Furthermore, the operating condition of the twin-screw extruder were simulated using the Carreau model for describing the flow behavior.

The viscosity values from this simulation were plotted as a function of chosen sampling sections.

The next step of this project will be the CFD model validation thanks to an experimental campaign on a scaled pilot plant, which is now under construction. This campaign will contemplate the viscosity evaluation in each sampling section identified during the computational analysis.

Once the validation will be done, the CFD model could be used for studying different screws geometries to find which configuration provides the best results in terms of product quality.

## ACKNOWLEDGMENTS

This work is partly supported by “POR-FESR 2014-2020, Emilia-Romagna Region, Asse 1: Ricerca e Innovazione - Bando per progetti di ricerca industriale strategica rivolti agli ambiti prioritari della Strategia di Specializzazione Intelligente - Progetto: Nuovi paradigmi per la progettazione, costruzione ed il funzionamento di macchine e impianti per l'industria alimentare”.

## REFERENCES

Ansys, Inc, (2009), Ansys Fluent Theory Guide. Chapter 8, Paragraph 4.5.

Bertrand, F., Thibault, F., Delamare, L., & Tanguy, P. A. (2003). Adaptive finite element simulations of fluid flow in twin-screw extruders. Computers & Chemical, 27, 491–500.

Cubeddu, A., Rauh, C., & Delgado, A. (2014). 3D Thermo-Fluid Dynamic Simulations of High-Speed-Extruded Starch Based Products. Open Journal of Fluid Dynamics, 04(01), 103–114.

Emin, M. a., & Schuchmann, H. P. (2012). Analysis of the dispersive mixing efficiency in a twin-screw extrusion processing of starch based matrix. Journal of Food Engineering, 115(1), 132–143.

Fabbri, A., Angioloni, A., Di Stefano, A., Fava, E., Guarnieri, A., & Lorenzini, G. (2012). Preliminary Investigation of Pasta Extrusion Process: Rheological Characterization of Semolina Dough. Journal of Agricultural Engineering, 38(2), 21–24.

Jamilah, B., Mohamed, A., Abbas, K. a., Abdul Rahman, R., Karim, R., & Hashim, D. M. (2009). Protein-starch interaction and their effect on thermal and rheological characteristics of a food system: A review. Journal of Food, Agriculture and Environment, 7(2), 169–174.

Lagarrigue, S., & Alvarez, G. (2001). The rheology of starch dispersions at high temperatures and high shear rates: A review. Journal of Food Engineering, 50(4), 189–202.

Messori, M. (2005). Tecnologie di Trasformazione dei Materiali Polimerici: Estrusione ed applicazione dell'estrusione. Stampaggio ad iniezione Soffiaggio di corpi cavi, 8(I).

Peressini, D. (2001). Evaluation methods of dough rheological properties. Tecnica Molitoria.

Rao, M. A., Okechukwu, P. E., Da Silva, P. M. S., & Oliveira, J. C. (1997). Rheological behavior of heated starch dispersions in excess water: role of starch granule. Carbohydrate Polymers, 33(4), 273–283.

Xie, F., Yu, L., Su, B., Liu, P., Wang, J., Liu, H., & Chen, L. (2009). Rheological properties of starches with different amylose/amylopectin ratios. Journal of Cereal Science, 49(3), 371–377.

Yamsaengsung, R., Noomuang, C., Law, H., Law, B., Law, B., Law, C., Extruder, a S. S. (2010). Finite Element Modeling for the Design of a Single-Screw Extruder for Starch-Based Snack Products. Engineering, III, 8–11.

## AUTHORS BIOGRAPHY

**Giorgia TAGLIAVINI** is a Research Assistant at the Department of Industrial Engineering at the University of Parma, where she graduated in Mechanical Engineering in March 2015. Her research activities focus mainly on CFD simulation and process modeling of Industrial and Food Engineering processes.

**Federico SOLARI** is a PhD in Industrial Engineering at the University of Parma, from where he got a Master degree in Food Industry Mechanical Engineering, discussing a thesis related to the design of a plant for the volatile compounds extraction. He achieved his PhD with a thesis entitled "Advanced approach to the design of industrial plants by means of computational fluid dynamics". He attended several conferences related to food process, modelling and simulation. He published several papers on the same topics on international journal and conferences.

**Roberto MONTANARI** is a Full professor of Mechanical Plants at the University of Parma. He graduated (with distinction) in 1999 in Mechanical Engineering at the University of Parma. His research activities mainly concern equipment maintenance, power plants, food plants, logistics, supply chain management, supply chain modelling and simulation, inventory management. He has published his research in approx. 70 papers, which appear in qualified international journals and conferences. He acts, as a referee, for several scientific journals, is editorial board member of two international scientific journals and editor of a scientific journal.